

STUDY OF STRUCTURE AND DYNAMICS OF GELATIN GELS BY
TEMPERATURE RAMPED HOLOGRAPHIC RELAXATION SPECTROSCOPY

Chi Wu , Wolfgang Schrof, Dieter Lilge
Erik Lüddecke and Dieter Horn

BASF AG, Polymer Research Division
Department of Polymer Physics & Solid State Physics
D-6700 Ludwigshafen/Rhine, Federal Republic of Germany

Abstract: A technique combined temperature ramp with holographic relaxation spectroscopy (HRS) is used to investigate on the structure and dynamics of gelatin gels. Two kinds of photochromic probes are used. The first is the gelatin molecule covalently labeled with fluorescein-isothiocyanate. After gelation, some of the labeled gelatin molecules will form the gel and the rest will still be in the sol. Therefore, the mobility of labeled gelatin molecules in the sol and the gel are probed. The translational diffusion coefficient of gelatin molecules in the sol, the gel content and the gel melting temperature at different gelatin concentrations ranging from 1 to 15 weight-% are measured. The second probe is the small fluorescein molecule in the gelatin gel as a tracer. The mobilities of the tracer in the "gel" are probed. An HRS curve with double peaks is observed. It is experimentally proven that this "anomalous" HRS curve is related to the structure of the gelatin gels. During a normal cooling process (2 °C/min), two kinds of networks are found. A "coarse" one is formed through the aggregation of collagen-like triple-stranded helices and a "fine" one is formed simply by entanglements between gelatin molecules.

INTRODUCTION

The conformational changes of gelatin in solution, the sol-gel transition, and the rheological properties of gelatin gels have aroused tremendous scientific interest over many decades, and are still under investigation (Ref.1-11). During the last ten years, a number of optical methods have been developed, which are based on measurements of the mobility of sensor molecules inside polymer networks (Ref.10-22). One such method, holographic relaxation spectroscopy (HRS), also known as forced Rayleigh scattering (FRS), was successfully applied to gelatin gels by Chang and Yu (Ref.10) in 1986, and the mobility of gelatin molecules inside the gelatin networks were reported and compared with results from dynamic light scattering. Later, Russo et al (Ref.11) reported a temperature-ramped fluorescence photobleaching recovery (TRFPR) technique to study gelatin gels.

In this work, a technique combining a temperature ramp with holographic relaxation spectroscopy (TR-HRS) (Ref.22) was used. In TR-HRS, the gelatin molecules are covalently labeled with fluorescein-isothiocyanate. After gelation, some of the labeled gelatin molecules will form the gel and the rest will still be in the sol. Therefore, the mobility of the labeled gelatin molecules in the sol and the gel are probed. In TR-HRS, there exist two kinds of relaxation processes. The first is processed before the temperature ramp through the translational diffusion of the gelatin molecules in the sol. When the temperature is ramped beyond T_m , the second relaxation is forced to occur because the immobile network starts to break into mobile fragments, such as microscopic gels, collagen-like triple- stranded helices and eventually gelatin molecules. From the first kind of relaxation process, the gel content and the mobility of gelatin molecules in the sol can be obtained quickly and directly by measuring the extent and rate of the HRS intensity relaxation. In TR-HRS, T_m can be measured from the intensity relaxation profile without introducing any kind of mechanical or chemical perturbation of the gel. Based on the observed gel content versus the setting time, it is found that the gelation process is first order, apparently in disagreement with other investigations (Ref.6,23-26). In addition, the mobility of the small fluorescein molecule in the gels was also investigated by HRS. It is found that there are two kinds of networks ("coarse" and "fine") existing in the gelatin gel when using a normal cooling process (1 °C/min). A "coarse" one is formed through aggregation of collagen-like triple-stranded helices and a "fine" one is formed simply by entanglements between gelatin molecules.

EXPERIMENTAL PART

Materials: Gelatin used in this experiment was purchased from Deutsche Gelatin Fabrik Stoess & Co. GmbH. It was a pharma grade B-type gelatin (Bloom value 200), i.e., it was obtained from alkaline treated bone-stock. GPC measurements (courtesy of Dr. Klaus Brumer and Dr. Wilfried Babel, Deutsche Gelatine-Fabriken Stoess AG, Eberbach) showed that the weight-average molecular weight (M_w) and the number-average molecular weight (M_n) were 1.4×10^5 g/mol and 6.3×10^4 g/mol, respectively. Fluorescein and fluorescein-isothiocyanate were from Riedel-de Haën Co. and Serva Co., respectively. Both were used without further purification. The details of sample preparation can be found elsewhere (Ref.10,11).

TR-HRS experiments: Basically, TR-HRS is an HRS instrument combined with a temperature ramp device. The detailed description of TR-HRS and our instrumentation can be found elsewhere (Ref.9,10,15,19). For convenience of discussion, the basic principle of TR-HRS is described briefly.

By crossing two coherent laser beams (writing beams) within the sample for a very short time (20 ms is typical for all our experiments), a spatial modulation of refractive index and/or absorption coefficient, i.e., the optical grating, is artificially created via a photochromic reaction. After this writing pulse, the periodic concentration distributions of the reacted and unreacted molecules will gradually be smeared out by the translational diffusion of the molecules. This relaxation process can be followed directly by measuring the transient diffraction intensity with another laser beam (reading beam) passing through the optical grating at Bragg's angle. Since the reading beam is far from the absorption band of fluorescein-isothiocyanate, the diffraction intensity is mainly from the refractive index change, i.e., "phase HRS". Therefore, the reading beam can monitor the relaxation process without any perturbation, such as a heating or bleaching of the sample.

RESULTS AND DISCUSSION

Labeled Gelatin Molecule as probe: Figure 1 shows a typical TR-HRS spectrum (continuous line) with a ramp rate of 1 °C/min. In an ideal situation, the intensity after the ramp should first stay constant until the temperature reaches T_m and then drop after T_m , as presented by a dotted-line in Figure 1. The experimental TR-HRS spectrum is obviously different from the ideal one. The measured TR-HRS spectrum always has an remarkable increase in intensity as the temperature rises before reaching T_m and a following sharp drop after passing T_m . It has been experimentally proved that this unexpected increase in the intensity is related the change of diffraction efficiencies of the optical grating (Ref.19).

The inset in Figure 1 shows a typical initial part of TR-HRS spectrum. In general, the relaxation process measured by the output signal $I(V)$ of a photomultiplier can be represented by

$$I(t) = [s(t) + g(t) + B]^2 + C^2 \quad (1)$$

where $s(t)$ and $g(t)$ denote the electric field of the diffracted light from the "sol phase" and the "gel phase",

respectively. B and C are the coherent and incoherent background scattering, respectively. Further $s(t)$ can be expressed as $\sum S_i \exp(-D_i K^2 t)$, $i=1,2,\dots,N$, where D_i and S_i are the translational diffusion coefficient and the electric field of the diffracted light of the i th component of the optical grating in the sol, respectively, and $K (=2\pi/L)$ is a constant at a fixed fringe spacing (L) of the optical grating. Below T_m , $g(t)$ ($=G$) is a constant because the gelatin molecules in the "gel phase" are immobile. In our experiments, B and C were negligible in comparison with $s(t)$ and $g(t)$.

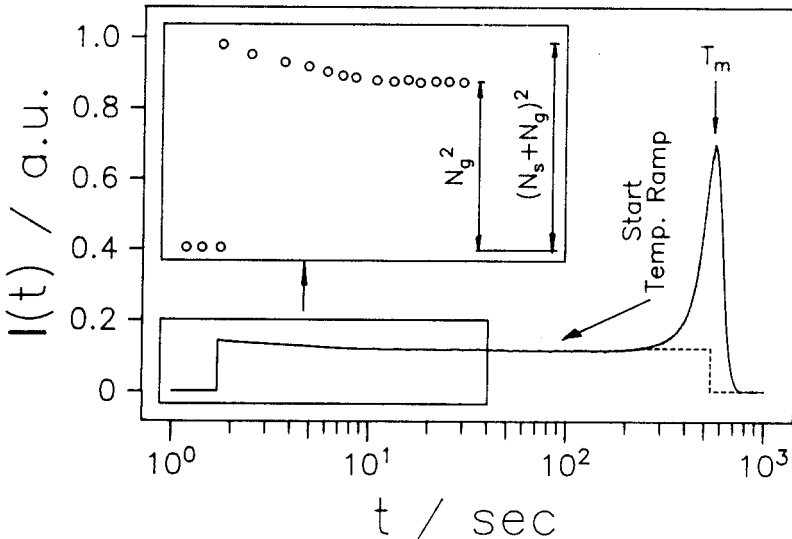


Fig.1. Typical TR-HRS spectrum (continuous line) of a 15 weight-% solution of the gelatin in buffer ($\text{pH} = 10$). Before the temperature ramp, the sample temperature was 25°C . The temperature-ramp rate is $1^\circ\text{C}/\text{min}$. Inset in the figure is the enlargement of the initial relaxation. The dotted-line represents an ideal TR-HRS spectrum after the temperature ramp. Y-axis is in arbitrary unit, denoted as "a.u." in all figures.

Based on Eq. (1) and a coupled wave theory (Ref.27) for a lossless transmission grating without slant, S and G are proportional to the amplitudes of the spatial modulation of the probe concentration (i.e., the number of probe molecules) provided the probe concentration is very dilute ($\sim 10^{-4}$ g/mL in

this study). Eq. (1) shows:

$$I(t) = P[N_s + N_g]^2 \quad \text{when } t = 0 \quad (2)$$

$$I(t) = P N_g^2 \quad \text{when } t \gg (D_i k^2) \quad (3)$$

where $N_s = \sum_i N_{s,i}$. Both $(N_s + N_g)^2$ and N_g^2 are shown schematically in the inset in Figure 1. The number concentration ratio of the gelatin molecules in the network (N_g) to the total gelatin molecules ($N_g + N_s$) in the sample is the so-called gel content, denoted as GC in the following discussions for simplicity.

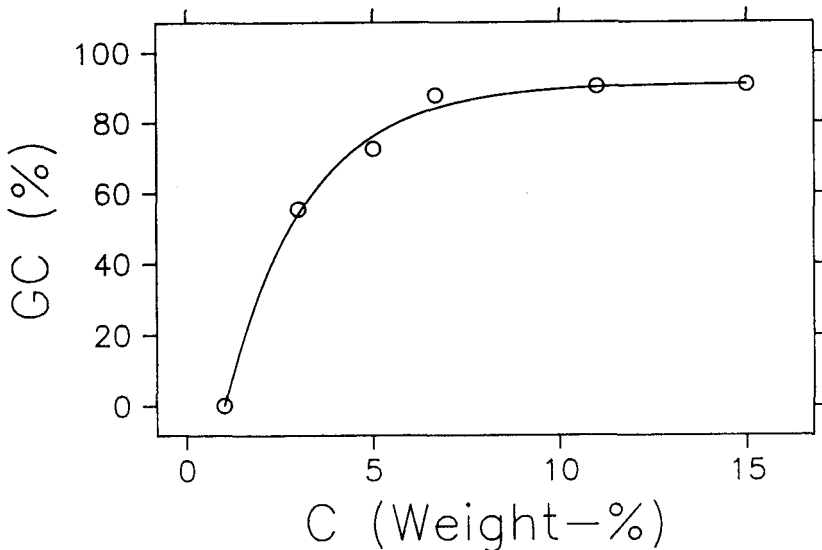


Fig.2. Concentration dependence of the gel content (GC) for the gelatin solution matured and measured at 25 °C. Open circles represent the experimental data and the continuous line shows a phenomenological fitting (see text for details).

Figure 2 shows how GC changes with the gelatin concentration (C). A phenomenological equation,

$$GC = a\{1 - \exp[-(C - C_0)/(C_c - C_0)]\} \quad (4)$$

was used for fitting the data, where C_0 is the concentration at which there is no gel in the sample and a is the gel

content when the concentration is 100 weight-%. Both the values of C_0 and a were experimentally predetermined to be 1% and 91%, respectively. Therefore, the fitting is simplified to a single parameter (C_c). The best fitting value of C_c is $(3.2 + 0.2)\%$, which is very similar to the overlap concentration, C^* ($\sim 3\%$) (Ref.28). Therefore, C_c is not only an empirical fitting constant, but also a characteristic gel concentration, i.e., only when the gelatin concentration is beyond C_c , there will be a measurable gel existing in the sample. This concept of a characteristic concentration should be general for various gels.

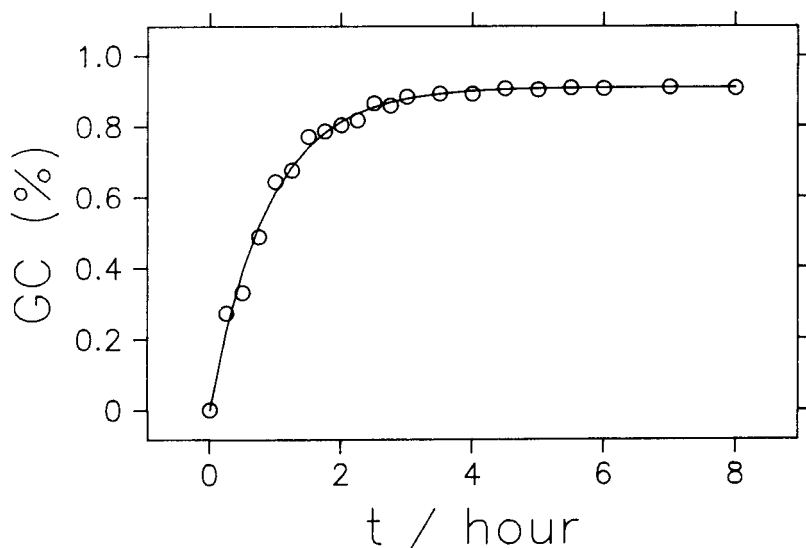


Fig.3. Kinetic study of the gel content (GC) for an 11 weight-% solution of gelatin in buffer (pH = 10) at 25 °C. Open circles represent the experimental data. (see text for details).

Figure 3 shows a kinetic study of gelation process. According to Harrington and Karr (Ref.26), the renaturation kinetics consists of three processes: nucleation, growth of triple-stranded helices and annealing. Each of them is a first-order reaction. They are parallel and summed to form an overall 3rd order reaction. The overall order of 3 has been confirmed by several other research groups (Ref.24,25). Our experimental results were analyzed by (Ref.29,30)

$$GC = GC_{\infty} [1 - \exp(-kt^n)] \quad (5)$$

where k is a rate constant, n the Avrami exponent and GC_{∞} the gel content at infinite setting time, experimentally determined as 91%. The experimental results were reasonably fitted by Eq. (5) with $k = 1.12 + 0.02 \text{ hour}^{-1}$ and $n = 1.0 + 0.1$ for the whole experimental time scale. The continuous line in Figure 3 represents the fitting. Hence, our experimental results suggest that the formation of networks in gelatin solutions be a first-order reaction. The first-order gel-formation kinetics can be understood because only the immobile molecules are considered as gel, and nucleation and the initial growth of triple-stranded helices cannot be observed using TR-HRS measurements. It is found that GC is proportional to the reciprocal of the setting temperature. By plotting GC versus $1/T$, a temperature ($T_{m,c}$), at which $GC = 0$, is obtained. $T_{m,c}$ is called the calculated gel-melting temperature in order to distinguish it from the directly measured T_m from TR-HRS spectrum. $T_{m,c}$ will be discussed later.

Naturally, T_m depends on the temperature-ramp rates. In TR-HRS, $0.5 \text{ }^{\circ}\text{C}/\text{min}$ seems to be a threshold temperature-ramp rate. When the ramp rate is faster than $0.5 \text{ }^{\circ}\text{C}/\text{min}$, T_m increases linearly with the ramp rate. When the rate is less than $0.5 \text{ }^{\circ}\text{C}/\text{min}$, T_m is constant to within uncertainties in the measurements. It is this T_m , measured with a ramp rate lower than the threshold rate, that was taken as the gel melting temperature.

T_m as described was checked against a visually measured gel temperature, $T_{m,visual}$. In the visual method, the flowing ability of a tilted gel at different test temperatures is observed. The three kinds of gel-melting temperature have values in the order $T_{m,c} < T_{m,visual} < T_m$, with the maximum difference between $T_{m,c}$ and T_m of about $1 \text{ }^{\circ}\text{C}$. Russo et al (Ref.11) also found that $T_{m,visual}$ is generally lower than T_m . One possible explanation for this difference is the "flow" observed in the visual method involves only breakage of the macroscopic gels, while TR-HRS measures "flow" within the scale of 5 - 50 μm . It seems that, at T_m , macroscopic gels are first broken into microscopic gels, then the microscopic gels continue to break into triple-stranded helices, and, finally, some of the helices break into gelatin molecules. At T_m , it usually takes hours to complete the whole melting process. Thus, lower ramp rates will provide more chance for gels to break at relatively lower temperatures. It is also true that lower ramp rates will provide more time for the fragments of

the broken gels to diffuse and separate. Hence $T_{m,c}$ has the lowest value because a gelatin sample for GC measurements is matured for at least 17 hours, providing a much higher chance for breakage of the gel, especially when the maturing temperature is very close to T_m .

It is also reasonable to assume that a macroscopic gel breaks at a lower temperature because there are always some weak linkages which require less energy to break. Thus, T_m is not a unique temperature. The measured T_m is always an average value, which changes with gelatin sample, concentration, setting temperature, measurement method, etc. For example, Figure 4 shows how T_m depends on gelatin concentration (C).

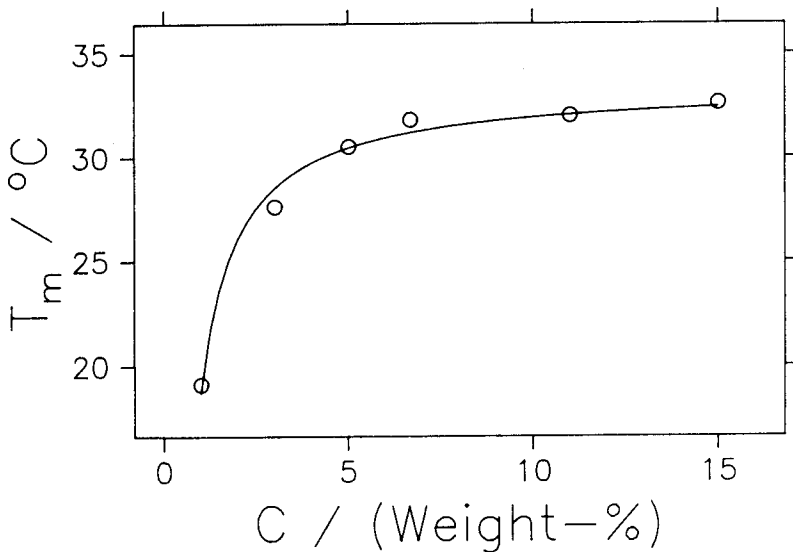


Fig.4. Concentration dependence of the measured gel melting temperature (T_m). Before measuring T_m , the samples were matured at 25 °C until the gel content reached a constant value. Open circles represent the measured T_m and the continuous line an empirical fitting (see text for details).

The continuous line in Figure 4 is a fitting of the experimental results using the empirical equation:

$$T_m = 33.4 \exp(-0.0044/C). \quad (6)$$

The mean translational diffusion coefficient (D) of gelatin

molecules in the sol can be calculated from the initial relaxation of TR-HRS curve by using the methods of cumulants or the inverse Laplace transform programs such as CONTIN (Ref.31), MSVD (Ref.32), etc. Figure 5 shows the concentration dependence of D . Basically, when C is higher than C_c , the value of D is approximates $7.3 \times 10^{-12} \text{ m}^2/\text{sec}$. This behavior suggests that the network has much less effect on the mobility of gelatin molecules in the sol. A similar observation has also been reported by other investigators (Ref.11). It is not well understood.

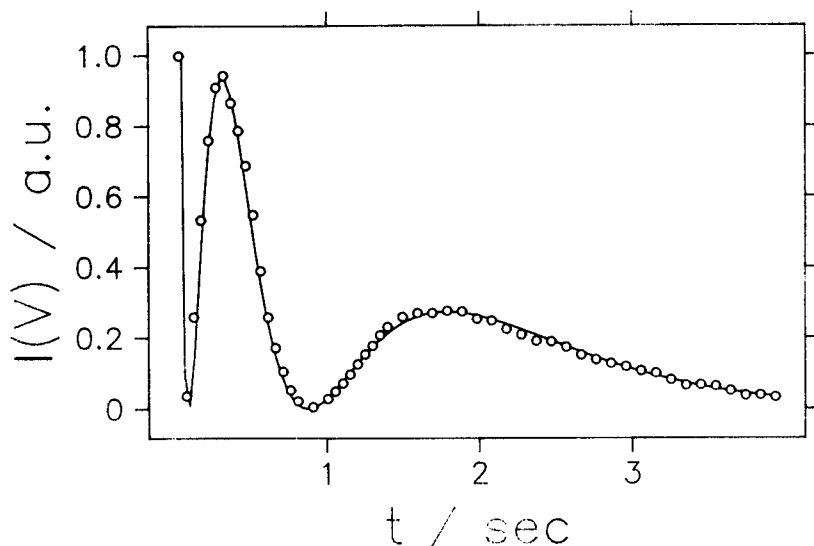


Fig.5. Concentration dependence of the mean translational diffusion coefficient (D) of gelatin molecules in the sol for samples matured and measured at 25°C . D was calculated by a second-order cumulant fitting. The uncertainty in D is 7.5%, which was difference between the repeat measurements.

Fluorescein as probe: an HRS curve with double peaks was found for gelatin gels formed by cooling gelation solutions from 50°C to 25°C at a rate of $\sim 2^\circ\text{C}/\text{min}$. The open circles in Figure 6 show such an experimental HRS curve. The reasons for this "anomalous" HRS curve could be that the gelatin gel is not uniform microscopically, but is a blend of "coarse" and "fine" networks. Each network will provide fluorescein molecules with one local "environment" because the average mesh size in the

"coarse" network is larger than the one in the "fine" network. That is, the microviscosities in these two networks are different and the translational diffusion coefficients of the fluorescein molecules will be different. For each "environment", the writing laser beam will create one pair of optical gratings with a phase shift of 180° , i.e., the prefactor S_i in Eq. (1) has the opposite sign. In total, the writing beam creates four sets of optical gratings. The curve in Figure 6 represents a best least squares fitting by using Equation (1) with $N = 4$ and the term $g(t)$ omitted because the small fluorescein molecule is not attached to the gel. The fitting is not unique because the resolution of sums of exponential functions is an ill-conditioned mathematical problem. Before the fitting parameters are taken seriously, the assumption of the two-environments has to be well-justified.

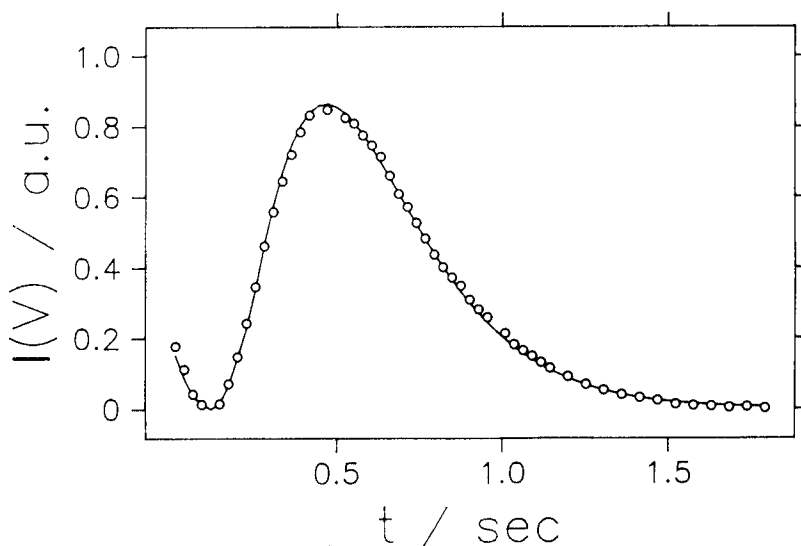


Fig.6. Typical HRS curve of a 15 weight-% gelatin gel prepared by cooling a solution of gelatin in buffer (pH = 10) from 50°C to 25°C at a rate of $1^\circ\text{C}/\text{min}$. The sample was matured and measured at 25°C . Open circles represent the experimental data and the continuous line represents a best-fitting using Equation (1) with $N = 4$.

If the two-environments assumption is correct, the HRS curve

measured at a high temperature ($\gg T_m$) should lack the anomalous double peaks because the "coarse" network will melt. The open circles in Figure 7 show an HRS curve at 60 °C for the same sample as in Figure 6. This decay-growth-decay spectrum is expected because there is only one "environment" in the sample when $T \gg T_m$. The curve in Figure 7 shows a best fitting by using Eq (1) with $N = 2$.

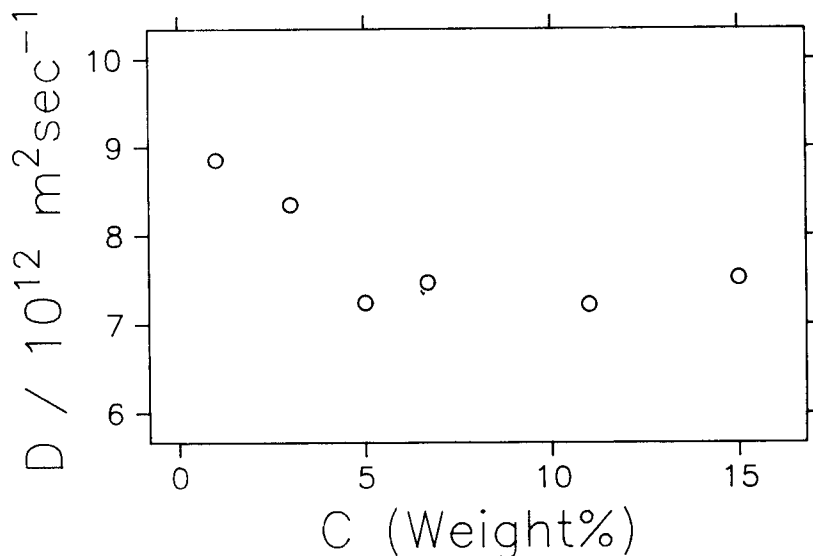


Fig.7. HRS curve for the same sample as in Figure 6. All experimental conditions were identical, except the measuring temperature was 60 °C instead of 25 °C. The gel melting temperature (T_m) was ~32 °C.

In order to confirm further the assumption of "two network environments" as a basis for explaining the spectrum in Figure 6, two samples were prepared and cooled from 50 °C to 25 °C at different rates. According to Stainsby (Ref.1), if the cooling rate is extremely low, the gelatin will have more opportunity to form the triple-stranded helices, and the gel will consist mostly of the "coarse" network. In contrast, in a quick-cooling process, there is not enough time for the gelatin molecules to form triple-stranded helices and the solution will be "frozen" into a "fine" network structure through entanglements between the polymer chains. Figure 8 shows the cooling-rate dependence of HRS curves. The continuous curve

represents a very slow cooling rate of $1\text{ }^{\circ}\text{C}$ per day and the broken curve a quickly-quenched sample. In Figure 8, the curve of the slowly cooled sample represents a diffusion process similar to the "fast" one in Figure 6 and the curve of the quenched sample represents a diffusion process similar to the "slow" one in Figure 6, in agreement with the previous interpretation of the results in Figure 6.

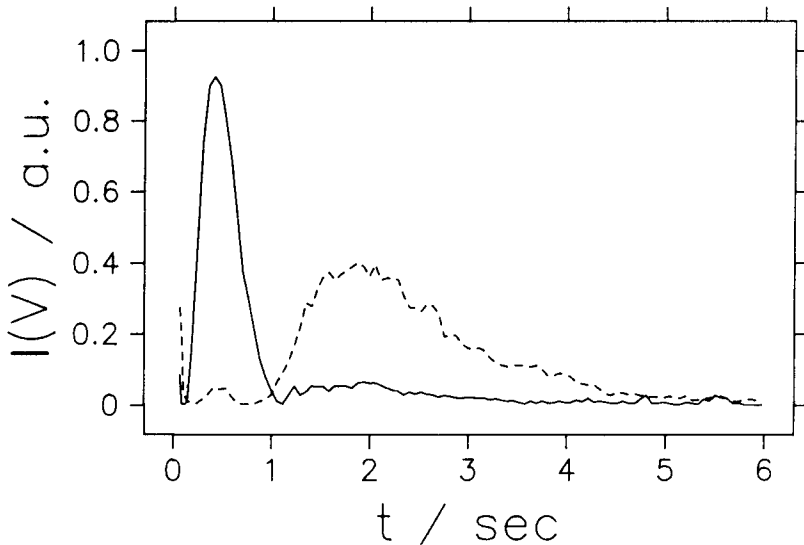


Fig.8. HRS curves for two gelatin gels prepared at different cooling rates, but with the same gelatin concentration (15 weight-% in the buffer). The continuous curve is for a sample prepared at a cooling rate of $1\text{ }^{\circ}\text{C}$ per day from $50\text{ }^{\circ}\text{C}$ to $25\text{ }^{\circ}\text{C}$ and the broken curve is for a sample quenched from $50\text{ }^{\circ}\text{C}$ to $25\text{ }^{\circ}\text{C}$ within 5 min.

Combining all the experimental results in this study, we conclude that, inside gelatin gels, there exist two kinds of local environments for the diffusion of fluorescein molecules. The observed anomalous feature in the HRS curve of gelatin gels arises from these two environments. Recently, Yu et al (Ref.9) also used HRS to study the dynamic structure of gelatin networks with a much larger tracer molecule, a photochromic labeled polyelectrolyte. They also observed two components of D below the gelation temperature. Finally, it should be emphasized that our results and discussion may be

valid only for certain gelatin samples because samples change dramatically from one source or method of preparation to another. The general validity of some of the empirical equations used in this article has to be checked before applying them to other gelatin samples and experimental conditions. In addition, some of the interpretations given in the discussion should be further verified using other experimental methods. However, the methodology reported in this article should be generally valid for reversible gels.

ACKNOWLEDGMENT

Chi Wu gratefully acknowledges the award of a Research Fellowship from the Alexander von Humboldt-Stiftung and the warm hospitality from BASF Aktiengesellschaft during his stay in Germany. The authors are indebted to Dr. Klaus Brumer and Dr. Wilfried Babel, Deutsche Gelatine-Fabriken Stoess AG, Eberbach, for the GPC measurements, and to Mr. Kren for preparing the samples and assisting with the measurements.

REFERENCES

- (1) A.G.Ward, A.Courts, The Science and Technology of Gelatin Academic press: London (1977)
- (2) A.Veis, The Macromolecular Chemistry of Gelatin, Academic press: London (1964)
- (3) M.Djabourov, Contemp. Phys., 29(3), 273 (1988)
- (4) M.E.Newcomer, T.A.Jones, J.Aqvist, J.Sundelin, U.Eriksson L.Rask, P.A.Peterson, EMBO J., 3(7), 1451 (1984)
- (5) C.Quellet, H.F.Eicke, R.Gehrke, W.Sager, Europhys. Lett., 9(3), 293 (1989)
- (6) W.Borchard, B.Luft, P.Reutner, J. Photoqr. Sci., 34(4), 132 (1986)
- (7) W.Borchard, K.Bergmann, A.Emberger, G.Rehage, Prog. Colloid. Polym. Sci., 60, 120 (1976)
- (8) M.Djabourov, P.Papon, Polymer, 24, 537 (1983)
- (9) H.Yoon, H.Kim, H.Yu, Macromolecules, 22, 848 (1989)
- (10) T.Change, H.Yu, Macromolecules, 17, 115 (1984)
- (11) P.S.Russo, M.Mustafa, D.Tipton, J.Nelson, D.Fontenot, Polym. Mater. Sci. Eng., 59, 605 (1988)
- (12) J.C.R.Williams, R.C.Daly, Prog. Polym. Sci., 5, 61 (1977)
- (13) H.Hervet, W.Urbach, F.Rondelez, J. Chem. Phys., 68(5), 2725 (1978)

- (14) J.A.Wesson, H.Takezoe, H.Yu, J. Appl. Phys., 53(10), 6513 (1982)
- (15) J.A.Lee, T.P.Lodge, J. Phys. Chem., 91, 5546 (1987)
- (16) J.Coutandin, H.Sillescu, Makromol. Chem. Rapid Commun., 3, 649 (1982)
- (17) B.A.Smith, E.T.Samulski, L.P.Yu, Phys. Rev. Lett., 52, 45 (1984)
- (18) U.Stewart, C.S.Johnson, D.A.Gabriel, Macromolecules, 19, 964 (1986)
- (19) T.C.Qui, T.Chang, C.Han, Y.Nishijima, Polymer, 27, 1705 (1986)
- (20) Chi Wu, W.Schrof, D.Lilge, E.Lddecke, D.Horn, Colloid Polym. Sci., in press.
- (21) J.Zhang, B.K.Yu, C.H.Wang, J. Phys. Chem., 90, 1299 (1986)
- (22) Chi Wu, W.Schrof, E.Lüddecke, D.Horn, Colloid Polym. Sci. accepted for publication.
- (23) P.V.Hauschka, W.F.Harrington, Biochemistry, 9, 3754 (1970)
- (24) K.te Nijenhuis, Colloid Polym. Sci., 259, 522 (1981)
- (25) D.D.Durand, J.R.Emery, J.Y.Chatellier, Int. J. Biol. Macromol. 7, 317 (1985)
- (26) W.F.Harrington, G.M.Karr, Biochemistry, 9, 3725 (1970)
- (27) H.Kogelnik, Bell Syst. Tech. J., 48, 2909 (1969)
- (28) R.Pecora, Dynamic Light Scattering, Plenum Press: New York, 217 (1985)
- (29) M.Avrami, J. Chem. Phys., 7, 1103 (1939); 2, 177 (1941)
- (30) R.Becker, Ann. Phys. (Leipzig), 32, 128 (1938)
- (31) S.W.Provencher, Biophys. J., 16, 29 (1976); J. Chem. Phys., 64, 2772 (1976); Makromol. Chem., 180, 201 (1979)
- (32) Chi Wu, W.Buck, B.Chu, Macromolecules, 20, 98 (1987)